Research Article | Vol. 28, No. 19 / 14 September 2020 / Optics Express 27727
Optics EXPRESS

Surface plasmon resonance effect on laser trapping and swarming of gold nanoparticles at an interface

CHIH-HAO HUANG,[1] TETSUHIRO KUDO,[1,6] ROGER BRESOLÍ-OBACH,[1,2,7] JOHAN HOFKENS,[2,3,8] TERUKI SUGIYAMA,[1,4,5,9] AND HIROSHI MASUHARA[1,5,10]

[1]*Department of Applied Chemistry, College of Science, National Chiao Tung University, Taiwan*
[2]*Laboratory for Photochemistry and Spectroscopy, Division for Molecular Imaging and Photonics, Department of Chemistry, Katholieke Universiteit Leuven, Belgium*
[3]*Max Planck Institute for Polymer Research, Mainz 55128, Germany*
[4]*Graduate School of Materials Science, Nara Institute of Science and Technology, Japan*
[5]*Center for Emergent Functional Matter Science, National Chiao Tung University, Taiwan*
[6]*kudo@nctu.edu.tw*
[7]*roger.bresoliobach@kuleuven.be*
[8]*johan.hofkens@kuleuven.be*
[9]*sugiyama@g2.nctu.edu.tw*
[10]*masuhara@masuhara.jp*

Abstract: Laser trapping at an interface is a unique platform for aligning and assembling nanomaterials outside the focal spot. In our previous studies, Au nanoparticles form a dynamically evolved assembly outside the focus, leading to the formation of an antenna-like structure with their fluctuating swarms. Herein, we unravel the role of surface plasmon resonance on the swarming phenomena by tuning the trapping laser wavelength concerning the dipole mode for Au nanoparticles of different sizes. We clearly show that the swarm is formed when the laser wavelength is near to the resonance peak of the dipole mode together with an increase in the swarming area. The interpretation is well supported by the scattering spectra and the spatial light scattering profiles from single nanoparticle simulations. These findings indicate that whether the first trapped particle is resonant with trapping laser or not essentially determines the evolution of the swarming.

1. Introduction

Laser trapping has been utilized as optical tweezers [1] in various research fields (e.g., biology or material sciences) for three-dimensional trapping and manipulation of nano- and micro-scale objects (e.g. nanoparticles (NPs), live cells, proteins, DNA, or small molecules, among others) [2]. Single metallic NP trapping in bulk solution was reported for different particle sizes from several to hundreds of nanometers [3,4]. Their high polarizability due to surface plasmon resonance (SPR) results in a larger trapping stiffness than typical dielectric NPs for the same particle size. Laser trapping of single Au nanorod and its orientation is controlled by the incident laser polarization with respect to its SPR [5]. Moreover, a shift of SPR band is spectroscopically observed for different laser power and polarization, when metallic NPs form an assembly inside the focal spot [6,7]. All these systems are examples of three-dimensionally trapped NPs inside the focal spot caused by a tightly focused laser beam when the gradient force is larger than scattering and absorption forces.

Laser trapping at an interface is considered to be a unique platform for assembling nanomaterials, where the optical potential and the induced assembly evolve outside the focal spot. For example, the formation of a highly concentrated molecular clusters domain (i.e., amino-acids)

#401158 https://doi.org/10.1364/OE.401158
Journal © 2020 Received 29 Jun 2020; revised 11 Aug 2020; accepted 28 Aug 2020; published 3 Sep 2020

Optics EXPRESS

around the trapping laser focus, leads to their crystallization only at solution surface and even for unsaturated solution [8–10]. When polystyrene NPs are trapped at the interface, a periodically aligned structure acts like a waveguide which allows the trapping laser to propagate and assemble more NPs beyond the focal spot [11,12]. A similar case is also observed for Au NPs, which form a dynamically fluctuating swarming assembly outside the focal spot [13]. For the initial stage, periodical structures (Yagi-Uda antenna like or hexagonal structures) are assembled inside the focal spot depending on the laser polarization (linear or circular, respectively). These structures are stabilized by an inter-particle radiation force, called optical binding [14], which is due to light scattering between the two particles. The observed configurations are in line with previous works on optical binding with metallic NPs [15–17]. For the stationary state, the dynamically fluctuating dumbbell-like swarms of Au NPs are evolved outside the focal spot, and its direction is perpendicular to the direction of linear polarization. We proposed that the trapping laser was scattered by trapped Au NPs towards the outside of the focus, and then further incoming NPs can be trapped and assembled outside the focal spot due to the optical binding. The assembling of NPs and light scattering are cooperatively and non-linearly developed, resulting in the swarming of Au NPs.

As a detail, the swarming is observed when 200 nm Au NPs are trapped by 1064 nm laser, which is resonant with the tail of its SPR band. Instead, the swarm is not found when the diameter of the NPs is smaller than 200 nm [13]. These facts suggest that the scattered light intensity needs to be higher than a certain value for the generation of swarming assemblies. Commonly, when the Au NP size decreases, the SPR band is blue-shifted, where the 1064 nm laser becomes off-resonance with respect to the SPR band. Therefore, the swarming assembly for smaller Au NPs should be observed by blue-shifting the laser wavelength toward the SPR band, as well as, a larger swarm could be achieved when it is exactly resonant to SPR band. It is worth mentioning that swarming is a complex system where a high number of Au NPs optically interact with each other through multiple light scattering. Moreover, the swarming phenomenon is coupled with Brownian motion, hydrodynamic interaction, photothermal heating and so on [18,19]. Among these complexities, the swarming is originated from the scattered light of Au NPs, which is strongly affected by its inherent SPR. In the present work, we focus on the effect of SPR-enhanced light scattering on the swarming phenomena.

2. Experiments

The experimental setup for laser trapping at the interface is illustrated in Fig. 1. Three different independent laser lines (640, 800, and 1064 nm) are separately introduced into an inverted microscope (Olympus, IX71). The laser power is controlled by a combination of a half-wave plate and a beam splitter or by neutral density filters. The laser beam size is enlarged using a beam expander to fill up the back aperture of an air-immersion objective lens (60 times magnified, NA 0.9, Olympus). The laser is reflected by a dichroic mirror inside the microscope body and focused by the objective lens. A halogen lamp is used as a light source for illuminating the sample through a dark-field condenser lens (NA 1.2-1.4; Olympus). The scattered light is collimated by the objective and guided towards the camera, where the backscattering of the trapping laser is filtered using a short-pass filter. The scattered light images are recorded by a charge-coupled device (CCD) or scientific Complementary Metal–Oxide–Semiconductor (sCMOS) camera. The laser power is set to 10 mW after the objective lens, where the adhesion of Au NPs to a glass substrate or aggregate formation due to heating and/or ablation can be avoided. When the NPs rarely adhere to the glass surface after a long irradiation time, we slowly shifted the stage of the microscope to avoid the adhesion effect on swarming.

The Au NPs used are commercially available with nominal diameter sizes of 100, 150, and 200 nm (BBI solutions). The particle concentration of each sample is normalized to 6×10^{-3} particles/μm^3. The Au colloidal solution is sonicated for 10 min, and then 15 µL of the suspension

Optics EXPRESS

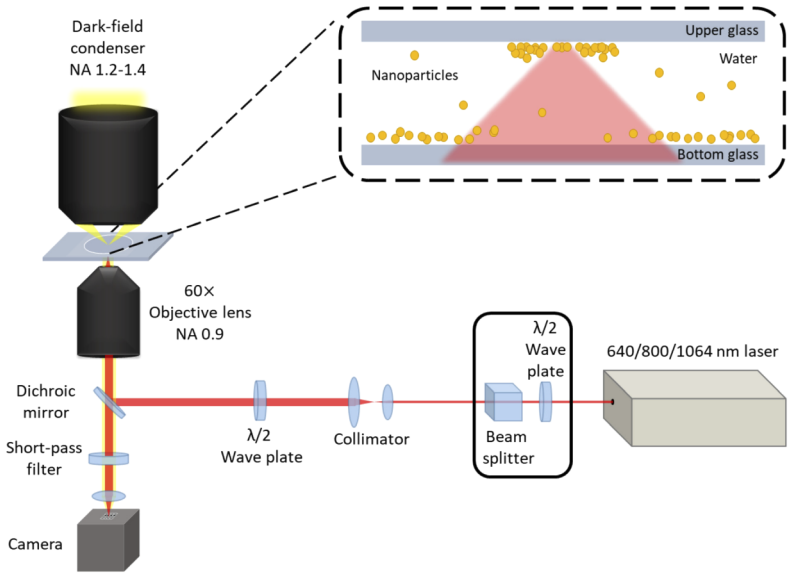

Fig. 1. Experimental setup for laser trapping of gold nanoparticles at an upper glass/solution interface. The dashed-line inset shows the illustration of sample a substrate containing the gold nanoparticles solution, in which the trapping laser is focused at the upper glass/solution interface.

is quickly sandwiched between two clean coverslips with a spacer (Electron Microscopy Sciences). The used coverslips are cleaned with a 5% solution of detergent (Hellmanex III, Hellma). The thicknesses of the chamber are approximately 100 μm.

3. Results and discussion

Upon laser irradiation, the Au NPs located on the bottom of the chamber are lifted up along the laser light propagation upward to focus, as we reported previously [13,20]. For 200 nm Au NPs with 1064 nm laser, it takes about 3 min for a first NP to arrive at the upper interface and be trapped at the focus (Fig. 2(a-i)). Then, the next few incoming particles always align linearly in the direction perpendicular to the laser polarization, and its interparticle distance (see Fig. S1 in Supplement 1) corresponds to the trapping laser wavelength in water (Fig. 2(a-ii)). After about 7 min of irradiation, the incoming Au NPs almost fully occupy the focal spot, and they start to expand outside the focal spot, where the incident laser is not directly shined (Fig. 2(a-iii)). Meanwhile, the periodically aligned structure of Au NPs like the Yagi-Uda antenna [21,22] is arranged at the focus, which constructively and directionally scatters the incident laser outside the focus. We proposed that this scattered light further optically bound the Au NPs outside the focus. With irradiation time increases, more Au NPs are trapped and further scatter the light, expanding the optical potential outside the focus. Thus, two swarms of fluctuating Au NPs are prepared at both sides of the focal spot, showing a dumbbell-like swarming assembly (Fig. 2(a-vi)). Such swarming is not observed when the NP size is reduced to 150 nm (Fig. 2(b)), although the linear alignment of 150 nm Au NPs perpendicular to laser polarization is observed at the initial stage. The obtained morphology is slightly ellipsoidal (Fig. 2(b-iv)) with small elongation along the direction perpendicular to laser polarization (Fig. 2(b-v)). When the assembly size is saturated after the 30 min (compare the assembly size in Figs. 2(b-v) to 2(b-vii)), the incoming rate of new NPs to focal spot and a rate of the NP diffusing outside the optical potential are balanced. Even

Optics EXPRESS

these incoming particles continuously reach the interface after saturation, they are not extended outside the focal spot. All these results are consistent with our previous report [13].

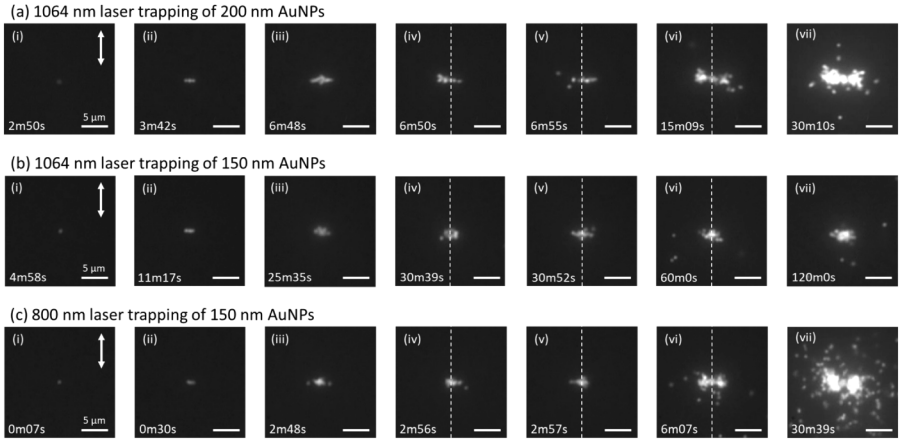

Fig. 2. Sequential scattering images of gold nanoparticles assemblies formed by linearly polarized trapping laser at the upper glass/solution interface. (a) 1064 nm laser trapping of 200 nm gold nanoparticles. (b) 1064 nm laser trapping of 150 nm gold nanoparticles. (c) 800 nm laser trapping of 150 nm gold nanoparticles. The direction of laser polarization is shown as white arrows. The vertical white dashed lines represent the central line where the focal spot is crossed. The length of all the white scale bars is 5 μm. See Visualization 1, for the formation of the swarming assembly for each condition.

Interestingly, the directional expansion and dumbbell-like swarming are observed for 150 nm Au NPs, when the laser wavelength is changed from 1064 to 800 nm as shown in Fig. 2(c-vii). The first Au NP is trapped in less than 10 s (Fig. 2(c-i)), and when more particles are trapped, they arranged accordingly to a linear alignment (Fig. 2(c-ii)). After a while (Fig. 2(c-iii)), the obvious dumbbell-like assembly for 150 nm Au NPs is achieved (see Visualization 1 for detail). To estimate the scattered light intensity from the single NP, we simulated the scattering spectra for each Au NP size in water according to Mie scattering theory [23] and plot in Fig. 3 together with the experimentally measured extinction spectra. It shows that the dipole mode of the SPR band is blue-shifted for smaller Au NPs sizes (compare Figs. 3(c) to 3(b)). Accordingly, when the Au NPs size is reduced from 200 to 150 nm, the scattering cross-section for 1064 nm trapping laser also decreases, leading to the suppression of swarming for the smaller-size NPs. The scattered light is enough to slightly elongate the assembly, although it is insufficient to form the dumbbell-like swarming outside the focal spot. Instead, when the 800 nm trapping laser is used, the scattering cross-section increases, and then the swarming is achieved. Furthermore, the swarming size for both conditions (200 nm Au NPs at 1064 nm wavelength and 150 nm Au NPs at 800 nm wavelength) is quite similar, which is in line with the similar value of the simulated scattering cross-section (6.0×10^4 and 4.8×10^4 nm^2, respectively).

A larger swarming assembly was observed with 200 nm Au NPs using 800 nm trapping laser, as shown in Fig. 4(b-iii) (also see Visualization 2). The swarm area is enlarged about 1.5 times compared to the swarm of 150 nm Au NPs. In this case, the 800 nm trapping laser almost matches the peak of the SPR dipole mode band, yielding a scattering cross-section approximately 2.7 times higher than the former case. We also conduct the laser trapping of 100 nm Au NPs, observing a small assembly inside the focal spot. Although swarming is not observed for both 1064 nm and 800 nm trapping laser, the assembly size for 100 nm Au NPs with 800 nm trapping laser is larger than with 1064 nm. The above described findings strongly support the role of the scattering cross-section on the swarming assembly formation and its size in the saturation stage.

Optics EXPRESS

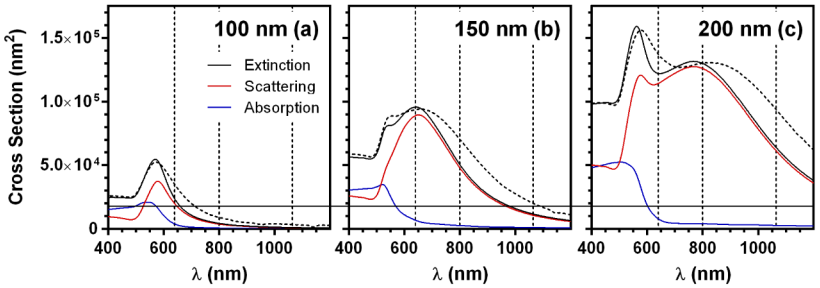

Fig. 3. Simulated extinction, scattering, and absorption spectra of single gold nanoparticle in water (black, red, and blue solid lines respectively). As a control, the experimental extinction spectra of gold nanoparticles in bulk solution are recorded, normalized and plotted as black dash lines. (a-c) The particle diameters are 100, 150, and 200 nm, respectively. The trapping laser wavelengths of 640, 800, and 1064 nm are marked as vertical dash lines in each plot. The horizontal solid black line refers to the scattering cross-section of 100 nm gold nanoparticle at 640 nm wavelength.

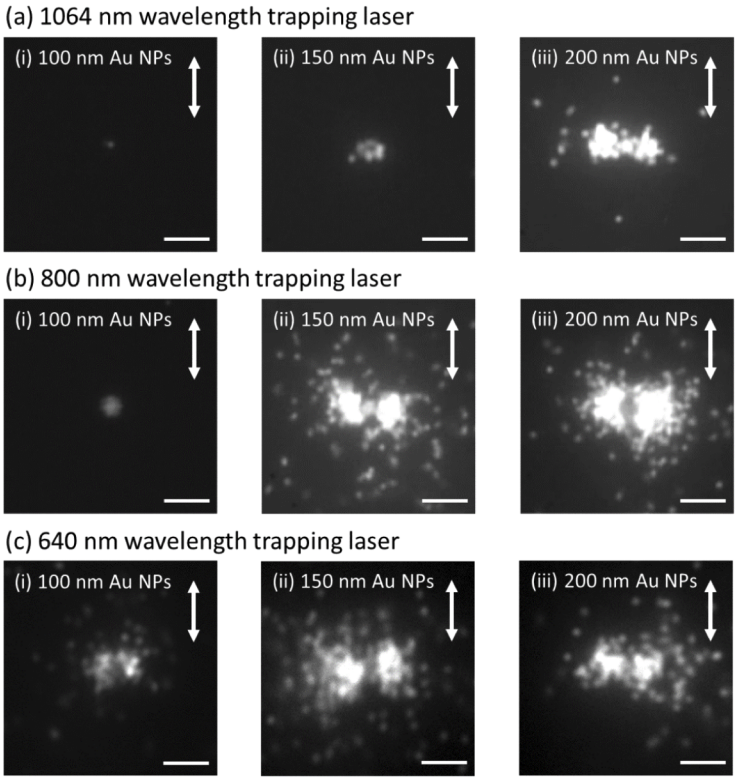

Fig. 4. Particle size and laser wavelength dependencies of gold nanoparticles assemblies formed by laser trapping. Each image is captured after 30 min of laser irradiation when the assembly size is saturated. The particle size is (i) 100, (ii) 150, and (iii) 200 nm in diameter, and the trapping laser wavelength is (a) 1064 nm, (b) 800 nm, and (c) 640 nm. The direction of laser polarization is shown as white arrows. The length of all the white scale bars is 5 μm. See Visualization 2, for the motion of the swarming assembly for each condition.

Optics EXPRESS

To further confirm the importance of the scattering cross-section, we have also tested even shorter trapping laser wavelength (640 nm). We observe the formation of swarming assemblies for all the tested Au NPs sizes (Fig. 4(c)). As explained above, the experimental conditions, where the swarming phenomenon is not observed, have scattering cross-sections in the range of 7.8×10^2–1.1×10^4 nm^2. These values are much smaller than the simulated ones for 640 nm. Therefore, we propose that the light scattering intensity (cross-section) of single NP should be higher than a certain value, 2.0×10^4 nm^2 under present condition (shown as the horizontal line in Fig. 3), to produce swarming assemblies (see a classification of each assemblies' dynamic states summarized as a chart in Fig. S2 in Supplement 1). Moreover, the expected swarming size for 200 nm Au NPs at 640 nm should be bigger than that observed experimentally, according to its scattering cross-section. A closer inspection of the scattering spectrum reveals that the 640 nm laser can excite both dipole and quadrupole modes [24]. The bands attributed to the dipole (λ_{max} 776 nm) and quadrupole (λ_{max} 557 nm) modes have been resolved by spectrum deconvolution and we estimate that about 30% of the 640 nm absorbed photons undergo a quadrupole excitation (further details in Fig. S3 in Supplement 1). Generally, the quadrupole radiation direction is not perpendicular to the laser polarization. Besides, at the far-field, quadrupole scattering decays with the third-power dependence of distance, as opposed to the second-power decaying with the distance of dipole mode [25]. Both properties suggest that quadrupole mode scattering should be less efficient than dipole mode scattering and consequently the dumbbell-like swarming is essentially due to the dipole mode.

As a final piece of evidence, we performed Finite-Difference Time-Domain (FDTD) simulation to study how the trapping laser of respective wavelengths is scattered by each Au NP size in the focal plane (Fig. 5). For simulation, an incident laser with a focal diameter corresponding to each wavelength is focused at the center of a fixed single Au NP. The incident focused laser is scattered by the single Au NP perpendicularly to linear polarization, according to dipole scattering phenomena. Increasing particle size and/or blue-shifting laser wavelength leads to an increase in the scattered light intensity. Although FDTD calculation is based on single NP simulation, the obtained intensity distribution is similar to the experimentally obtained swarming area for all the tested conditions. Therefore, this correspondence confirms the key role of single-particle SPR scattering in swarming phenomena and points out FDTD as an excellent simulation method for designing new swarming assemblies. For the rigorous theoretical analysis, the simulation with a number of Au NPs and their dynamics under the tightly focused trapping laser expressed by sectoral multipole beams [26] is required as a future topic. In addition, how particle number and interparticle distance inside the swarms are coupled with local photothermal heating, Brownian motion, convection flow, and microfluidic interaction will also be clarified in the following work to understand the swarming phenomena fully.

We have discussed the importance of SPR effect on swarming on the basis of simulated scattering spectra and scattering patterns in a single NP level. It may be mentioned that the swarms are composed of many Au NPs which are vigorously moving. They may have chances to approach closer or even collide with each other, where the near-field interaction becomes significant enough to modify the optical properties [6,7,27,28]. However, the Au NPs inside the focus are separated perpendicular to the linear polarization with an interval reflecting the wavelength of the incident laser in medium, which is far enough to exclude the effect of near-field interaction. In addition, the electrostatic repulsion force should be large enough to avoid the formation of aggregates. We, therefore, suppose that the total scattered light intensity from the NP inside the focus is a summation of the light scattering from individual NPs, and the dumbbell-like swarms are formed when its individual NPs' light scattering is resonantly enhanced by tuning the laser wavelength near to their SPR band.

Optics EXPRESS

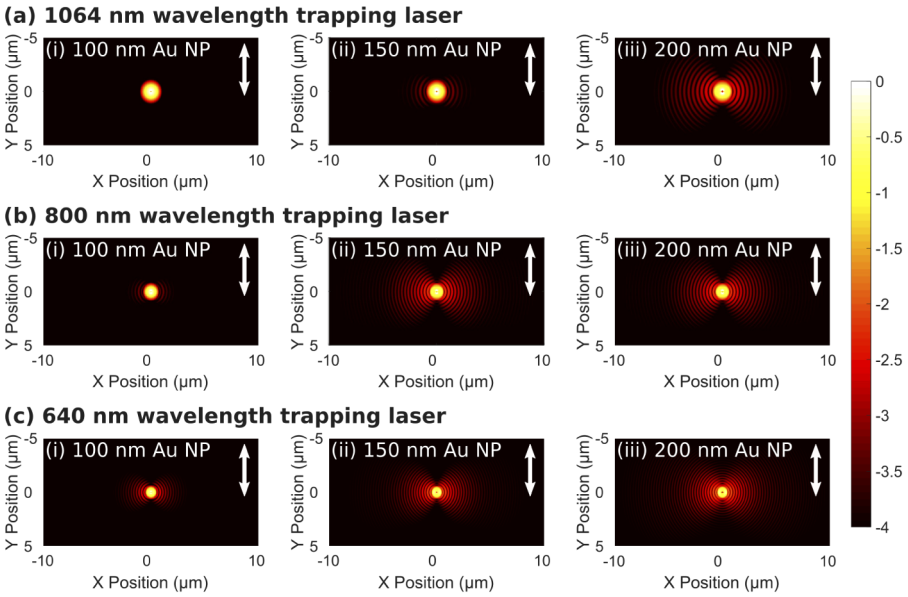

Fig. 5. FDTD simulation results showing the total intensity distribution of incident laser beam and scattered light from single gold nanoparticle situated in the focal spot. The scattering intensity is displayed in a logarithm scale, and the amplitude is normalized. The incident laser beam is propagated along z-direction and focused at the origin. The trapping laser wavelength is (a) 1064, (b) 800, and (c) 640 nm. The gold nanoparticle diameter is (i) 100, (ii) 150, and (iii) 200 nm. The direction of the linear laser polarization is shown as white arrows.

4. Conclusion

To conclude, we have studied the trapping and formation of Au NPs assemblies by tuning the trapping laser wavelength and/or the Au NP size to comprehensively understand the swarming phenomena in terms of SPR. The swarming is formed when the laser wavelength is near to the dipole mode of SPR (i.e., high scattering cross-section), while the swarming is not observed when the laser wavelength is far from the SPR band (i.e., low scattering cross-section). The observed behavior is well supported with the light scattering intensity profile calculated by FDTD simulation. The present findings clarify that the trapping laser is resonantly and strongly scattered by the first trapped Au NP due to its inherent SPR nature. Later, the scattered light incorporates more Au NPs and initiates the evolution of swarms outside the focal spot. The results obtained from the previous paper (where the swarming phenomena were reported for the first time) [13] suggested that SPR plays a role, however, this was not proved as no systematic study on the relationship between particle size and laser wavelength was carried out (only a single laser wavelength, 1064 nm, was used). In the present work, we clearly demonstrate how we can expand and control the formation of swarming assembly in a wider range of conditions by tuning the trapping laser wavelength with respect to the SPR band of the Au NPs with different sizes. Furthermore, our finding provides evidence which elucidates the underlying phenomena in swarming from the viewpoint of resonant oscillation of collective free-electron charges in metallic NPs. Recently, several works have reported nanoantenna structures for tailoring the direction of light scattering [29–34]. We believe that the swarming direction and morphology could be flexibly controlled by integrating these designed nanostructures. For instance, the nanoantenna for unidirectional light scattering will be self-organized by laser trapping at a nanostructure-patterned substrate providing unidirectional swarming.

Optics EXPRESS

Funding

Japan Society for the Promotion of Science (JP16H06507); Fonds Wetenschappelijk Onderzoek (G0B4915N,12Z8120N, V4138 20N); Flemish Government (CASAS2, Meth/15/04); Ministry of Education, Taiwan (Center for Emergent Functional Matter Science, The Higher Education Sprout Project of National Chiao Tung University); Ministry of Science and Technology, Taiwan (MOST 108-2112-M-009-008-, MOST 108-2113-M-009-011-, MOST 108-2113-M-009-015-, MOST 109-2634-F-009-028).

Acknowledgments

This work was supported by Ministry of Science and Technology (MOST) of Taiwan (MOST 108-2113-M-009-015- to H.M., MOST 108-2113-M-009-011- to T.S. and MOST 108-2112-M-009-008- to T.K.). J.H. gratefully acknowledges the financial support of the Flemish Government through long-term structural funding Methusalem (CASAS2, Meth/15/04), and from the Fonds Wetenschappelijk Onderzoek-Vlaanderen (G0B4915N). R.B.-O. thanks to the Fonds Wetenschappelijk Onderzoek-Vlaanderen for a postdoctoral (12Z8120N) and a long stay abroad (V4138 20N) fellowships. Thanks are also due to a grant from JSPS KAKENHI (Grant JP16H06507 in Scientific Research on Innovative Areas "Nano-Material Optical-Manipulation" to T.S.). H.M. and T.S. thank the Ministry of Science and Technology, Taiwan (Grant No. MOST 109-2634-F-009-028) and the Center for Emergent Functional Matter Science of National Chiao Tung University from The Featured Areas Research Center Program within the framework of the Higher Education Sprout Project by the Ministry of Education (MOE) in Taiwan.

This paper is dedicated to late Prof. Juan Jose Sáenz of Donostia International Physics Center in Euskadi (Spain) for his enthusiastic support to international collaboration on COODy-Nano (collective optofluidic dynamics of nanoparticles).

Disclosures

The authors declare no competing financial interest.

See Supplement 1 for supporting content.

References

1. A. Ashkin, J. M. Dziedzic, J. E. Bjorkholm, and S. Chu, "Observation of a single-beam gradient force optical trap for dielectric particles," Opt. Lett. **11**(5), 288–290 (1986).
2. D. Gao, W. Ding, M. Nieto-Vesperinas, X. Ding, M. Rahman, T. Zhang, C. Lim, and C.-W. Qiu, "Optical manipulation from the microscale to the nanoscale: fundamentals, advances and prospects," Light: Sci. Appl. **6**(9), e17039 (2017).
3. K. Svoboda and S. M. Block, "Optical trapping of metallic Rayleigh particles," Opt. Lett. **19**(13), 930–932 (1994).
4. P. M. Hansen, V. K. Bhatia, N. Harrit, and L. Oddershede, "Expanding the optical trapping range of gold nanoparticles," Nano Lett. **5**(10), 1937–1942 (2005).
5. M. Pelton, M. Liu, H. Y. Kim, G. Smith, P. Guyot-Sionnest, and N. F. Scherer, "Optical trapping and alignment of single gold nanorods by using plasmon resonances," Opt. Lett. **31**(13), 2075–2077 (2006).
6. Y. Tanaka, H. Yoshikawa, T. Itoh, and M. Ishikawa, "Laser-induced self-assembly of silver nanoparticles via plasmonic interactions," Opt. Express **17**(21), 18760–18767 (2009).
7. H. Yoshikawa, T. Matsui, and H. Masuhara, "Reversible assembly of gold nanoparticles confined in an optical microcage," Phys. Rev. E **70**(6), 061406 (2004).
8. T. Sugiyama, T. Adachi, and H. Masuhara, "Crystallization of glycine by photon pressure of a focused CW laser beam," Chem. Lett. **36**(12), 1480–1481 (2007).
9. T. Rungsimanon, K. Yuyama, T. Sugiyama, and H. Masuhara, "Crystallization in unsaturated glycine/D2O solution achieved by irradiating a focused continuous wave near infrared laser," Cryst. Growth Des. **10**(11), 4686–4688 (2010).
10. T. Sugiyama, K. Yuyama, and H. Masuhara, "Laser trapping chemistry: From polymer assembly to amino acid crystallization," Acc. Chem. Res. **45**(11), 1946–1954 (2012).
11. S.-F. Wang, T. Kudo, K. Yuyama, T. Sugiyama, and H. Masuhara, "Optically Evolved Assembly Formation in Laser Trapping of Polystyrene Nanoparticles at Solution Surface," Langmuir **32**(47), 12488–12496 (2016).

Optics EXPRESS

12. T. Kudo, S.-F. Wang, K. Yuyama, and H. Masuhara, "Optical Trapping-Formed Colloidal Assembly with Horns Extended to the Outside of a Focus through Light Propagation," Nano Lett. **16**(5), 3058–3062 (2016).
13. T. Kudo, S.-J. Yang, and H. Masuhara, "A Single Large Assembly with Dynamically Fluctuating Swarms of Gold Nanoparticles Formed by Trapping Laser," Nano Lett. **18**(9), 5846–5853 (2018).
14. M. M. Burns, J. M. Fournier, and J. A. Golovchenko, "Optical binding," Phys. Rev. Lett. **63**(12), 1233–1236 (1989).
15. Z. Yan, R. A. Shah, G. Chado, S. K. Gray, M. Pelton, and N. F. Scherer, "Guiding spatial arrangements of silver nanoparticles by optical binding interactions in shaped light fields," ACS Nano **7**(2), 1790–1802 (2013).
16. Z. Yan, S. K. Gray, and N. F. Scherer, "Potential energy surfaces and reaction pathways for light-mediated self-organization of metal nanoparticle clusters," Nat. Commun. **5**(1), 3751 (2014).
17. P. McCormack, F. Han, and Z. Yan, "Self-Organization of Metal Nanoparticles in Light: Electrodynamics-Molecular Dynamics Simulations and Optical Binding Experiments," J. Phys. Chem. Lett. **9**(3), 545–549 (2018).
18. R. Delgado-Buscalioni, M. Meléndez, J. Luis-Hita, M. I. Marqués, and J. J. Sáenz, "Emergence of collective dynamics of gold nanoparticles in an optical vortex lattice," Phys. Rev. E **98**(6), 062614 (2018).
19. I. Aibara, C.-H. Huang, T. Kudo, R. Bresolí-Obach, J. Hofkens, A. Furube, and H. Masuhara, "Dynamic Coupling of Optically Evolved Assembling and Swarming of Gold Nanoparticles with Photothermal Local Phase Separation of Polymer Solution," J. Phys. Chem. C **124**(30), 16604–16615 (2020).
20. T. Uwada, T. Sugiyama, and H. Masuhara, "Wide-field Rayleigh scattering imaging and spectroscopy of gold nanoparticles in heavy water under laser trapping," J. Photochem. Photobiol., A. **221**(2-3), 187–193 (2011).
21. T. Kosako, Y. Kadoya, and H. F. Hofmann, "Directional control of light by a nano-optical Yagi–Uda antenna," Nat. Photonics **4**(5), 312–315 (2010).
22. I. S. Maksymov, I. Staude, A. E. Miroshnichenko, and Y. S. Kivshar, "Optical Yagi-Uda nanoantennas," Nanophotonics **1**(1), 65–81 (2012).
23. B. K. Juluri, J. Huang, and L. Jensen, "Extinction, Scattering and Absorption efficiencies of single and multilayer nanoparticles," (Nanohub 2016). https://nanohub.org/resources/nmie
24. J. Rodríguez-Fernández, J. Pérez-Juste, F. Javier García de Abajo, and L. M. Liz-Marzán, "Seeded growth of submicron Au colloids with quadrupole plasmon resonance modes," Langmuir **22**(16), 7007–7010 (2006).
25. J. D. Jackson, *Classical Electrodynamics* (Wiley, 1999).
26. J. Olmos-Trigo, M. Meléndez, R. Delgado-Buscalioni, and J. J. Sáenz, "Sectoral multipole focused beams," Opt. Express **27**(11), 16384–16394 (2019).
27. G. Obara, N. Maeda, T. Miyanishi, M. Terakawa, N. N. Nedyalkov, and M. Obara, "Plasmonic and Mie scattering control of far-field interference for regular ripple formation on various material substrates," Opt. Express **19**(20), 19093–19103 (2011).
28. Y. Tanaka, G. Obara, A. Zenidaka, N. N. Nedyalkov, M. Terakawa, and M. Obara, "Near-field interaction of two-dimensional high-permittivity spherical particle arrays on substrate in the Mie resonance scattering domain," Opt. Express **18**(26), 27226–27237 (2010).
29. S. J. Oldenburg, G. D. Hale, J. B. Jackson, and N. J. Halas, "Light scattering from dipole and quadrupole nanoshell antennas," Appl. Phys. Lett. **75**(8), 1063–1065 (1999).
30. A. G. Curto, G. Volpe, T. H. Taminiau, M. P. Kreuzer, R. Quidant, and N. F. VanHulst, "Unidirectional emission of a quantum dot coupled to a nanoantenna," Science **329**(5994), 930–933 (2010).
31. L. Novotny and N. VanHulst, "Antennas for light," Nat. Photonics **5**(2), 83–90 (2011).
32. D. Vercruysse, Y. Sonnefraud, N. Verellen, F. B. Fuchs, G. DiMartino, L. Lagae, V. V. Moshchalkov, S. A. Maier, and P. VanDorpe, "Unidirectional side scattering of light by a single-element nanoantenna," Nano Lett. **13**(8), 3843–3849 (2013).
33. E. LeMoal, S. Marguet, B. Rogez, S. Mukherjee, P. DosSantos, E. Boer-Duchemin, G. Comtet, and G. Dujardin, "An electrically excited nanoscale light source with active angular control of the emitted light," Nano Lett. **13**(9), 4198–4205 (2013).
34. G. Lu, Y. Wang, R. Y. Chou, H. Shen, Y. He, Y. Cheng, and Q. Gong, "Directional side scattering of light by a single plasmonic trimer," Laser Photonics Rev. **9**(5), 530–537 (2015).